Chemisorption on Metal Surfaces: Cluster Model Studies [#]

Xin Xu,* Nanqin Wang, and Qianer Zhang

State Key Laboratory for Physical Chemistry in Surface Science, Department of Chemistry, Xiamen University,
Xiamen 361005, People's Republic of China

(Received April 13, 1995)

After exploring the underlying physics of the cluster-surface analogy, we propose the concept of "metallic atom". The importance of employing a metallic cluster in the cluster modeling of chemisorption is illustrated with some case studies.

In the cluster-surface analogy, the adsorbate species is presumed to interact with a single metal atom or a small group of metal atoms. Thus one obtains bonding and antibonding levels, reminiscent of the simple valence theory of diatomic molecules. However, it is evident that the applicability of methods and notions well proven in molecular chemistry can start to be questionable when a small cluster is used to simulate a solid surface. As pointed out by Muetteries and Wexler,[1)] "Coordination chemistry principles, especially those derived from molecular cluster chemistry, can be invaluable conceptually in attempts to delineate the molecular details of metal surface chemistry, provided that the application of such concepts is done with considerable caution and reserve". In this paper, we try to explore the underlying physics of the cluster-surface analogy. Emphasis is on what we can do and how we can proceed for a better cluster modeling of chemisorption. The significance of employing the concept of "meltallic atom" in the cluster approach to chemisorption on metals is illustrated with some case studies.

The Cluster-Surface Analogy

Here is a convenient scheme which elucidates the idea of the cluster-surface analogy, and which is always used as the starting point of a quantum calculation of chemisorption:[2)] (1) remove a substrate atom M from the surface; (2) the adsorbate L couples to this substrate atom M to form a cluster M–L; (3) either (a) embed M–L in the rest of the substrate, or (b) enlarge the size of the cluster M–L, M_2–L, $\cdots$, M_n–L, M_n cluster will tend to become surface when n approaches to infinity. Step 3 is considered to be the most difficult. Usually, a cluster of small size is used to simulate a surface.

There are two popular ways in cluster studies of chemisorption. One is to extend the size of the cluster as large as possible, the other is to utilize the molecular orbital theory as accurately as possible. However, although the increase of cluster size implies that the cluster tends to become a surface, it also means more computational difficulties and expenditure. Various simplifications have to be introduced to make calculations tractable, which in turn reduces the reliability and advantage of the large cluster calculations. On the other hand, the "accurate" calculations of a small cluster do give more details of the chemical interactions but a small cluster is too molecular to represent a surface. In short, one is faced with the dilemma that there are qualitative errors in a small cluster, whereas there are quantitative difficulties in a large cluster.[3)] Then WHAT can be done for a better cluster-surface analogy?

The Concept of Metallic Atom

In our opinion, the very important step (1) has been unfortunately ignored in the current cluster approach to chemisorption. Remember a substrate atom M is removed from the metal surface in step (1). Thus the substrate atom M taken from the bulk is an atom in the metallic state, which should possess the characteristic electronic properties of the bulk. In other words, the cluster atom in the cluster-surface analogy should be a "metallic atom" rather than a simple metal atom.

It is well known that in a Hartree–Fock calculation, the calculation results largely depend on the choices of geometry, multiplicity, and basis functions. Since the experimental results demonstrate that the free metal clusters have little in common with the geometries of bulk metal (e.g. Cr_2 0.168 nm[4)] vs. 0.249 nm in bulk[5)]), one usually use cluster geometries that are appropriate for bulk metal in the cluster-surface analogy. However there is little information regarding how to choose the multiplicities and basis functions according to the electronic properties of a bulk metal. Conventionally, the basis functions employed in a cluster model calculation are those optimized from certain atomic states, and the multiplicity of the model cluster is determined by the lowest total energy. For example, the atomic ground state of Pd is ^1S ($4d^{10}$),[5)] while the energy band calculation of bulk Pd indicate a metallic state of ($4d^{9.63}5sp^{0.37}$).[6)] The first ionization

---

#Supported by the National Natural Science Foundation of China.

potential of Pd atom is 8.3 eV,[5)] while the work function of bulk Pd is about 6 eV.[7)] Thus the most conventional choice of a closed shell configuration for Pd_n cluster modeling of bulk Pd is doubtful, and the applicability of atomic basis functions of ground state Pd atom to describe bulk Pd may be questionable. Then HOW can we proceed for a better cluster-surface analogy?

Case Studies

From the above discussion it is clear that not only the geometry, but also the multiplicity and basis functions of the model cluster should be appropriate for bulk metal in a cluster-surface analogy. Since CO chemisorbed on metal surface has been intensively investigated both experimentally and theoretically, we choose this system to explain our ideas. All our calculation results shown below are based on ab initio UHF method and Koopmans' theorem.

Metallic Basis Functions. The electrons in a bulk metal possesses two kinds of motion. One is within the atoms themselves, which retain much of the same character as in the isolated atoms. The other is called "the collective motion", which is specific for "metallic atoms". The electrons participating in collective motion can move quite freely through the assembly of nuclei and could be considered as "free electrons". Therefore the nucleus of a metallic atom is not only screened by its respective electrons but also screened by the free electrons coming from other atoms. The attractive potential in a metallic atom is[8)]

$$\varphi_{\mathrm{m}}(r) = -\frac{Z^*}{r}\mathrm{e}^{-k_{\mathrm{S}}r} \tag{1}$$

where $1/k_{\mathrm{S}}$ is the Thomas–Fermi screening length. In comparison, the potential energy in an isolated atom is

$$\varphi_{\mathrm{a}}(r) = -\frac{Z^*}{r} \tag{2}$$

Considering the computational and physical simplicity of STO-nG, we have constituted a set of metallic Slater bases. The so-called metallic Slater exponents ζ_{m} can be given as a modification of the atomic Slater exponents ζ_{a}:

$$\zeta_{\mathrm{m}} = \zeta_{\mathrm{a}} + \Delta\zeta \tag{3}$$

where $\Delta\zeta$ can be obtained from the free electron theory in solid state physics.

Table 1. Comparison between Metallic ζ_{m} and Atomic ζ_{a} of Co Atom

	1s	2sp	3sp	3d	4sp
ζ_{a}	26.47	11.09	4.55	3.94	1.40[9)]
ζ_{m}	26.46	10.96	4.01	3.35	1.84

For an internal shell, $\Delta\zeta$ is given by:

$$\Delta\zeta = -\frac{\rho(\zeta_{\mathrm{a}}(n))}{n} \tag{4}$$

while for the outermost valence-shell, $\Delta\zeta$ is:

$$\Delta\zeta = +\frac{\rho(\zeta_{\mathrm{a}}(n-1))}{n} \tag{5}$$

Here n is the principal quantum number, $\rho(\zeta_{\mathrm{a}}(n))$ is the number of screening free electrons with respect to $\zeta_{\mathrm{a}}(n)$, which is given by:

$$\rho(\zeta_{\mathrm{a}}(n)) = n\zeta_{\mathrm{a}}(n)\left[1-\left(1+\frac{nk_{\mathrm{S}}}{\zeta_{\mathrm{a}}(n)}\right)\mathrm{e}^{-nk_{\mathrm{S}}/\zeta_{\mathrm{a}}(n)}\right] \tag{6}$$

More detailed description of the modification procedure was given in Ref. 3.

Table 1 presents a comparison between the metallic ζ_{m} and atomic ζ_{a} of Co. From Table 1 it can be seen, that the maximum effect of modification is on the external valence electrons. This is in accord with the common knowledge of the behavior of electrons in the bulk. Table 2 summarizes the results of UHF/STO-3G calculation of Co. Although ζ_{a} gives a lower total energy, it fails to yield the correct number for the first ionization potential of the atomic Co. On the other hand, the HOMO levels calculated by the metallic ζ_{m} lie around 5.0 eV, which is in agreement with the metallic work function. Reasonable valence orbital levels of M should be an important factor to ensure the cluster-surface analogy.

Table 3 summarizes the computed ionization potentials of the electrons in the CO-like orbitals in M-CO with atomic ζ_{a} and metallic ζ_{m} where Koopmans' theorem is employed. The calculated IP's with atomic ζ_{a} are all more than 2 eV higher than the corresponding experimental values, while the calculated IP's with metallic ζ_{m} are in good agreement with the UPS data. The energy separation between the 1π and 4σ molecular orbitals is believed to be correlated with the

Table 2. UHF/STO-3G Calculations of Co Atom with ζ_{a} and ζ_{m}. * Indicates LUMO (au)

$2S+1=4$	10	11	12	13	14	15	16
Orbital energy							
α ζ_{a}	−0.2237	−0.1643	−0.1643	−0.1643	−0.1087	−0.1087	0.1344*
ζ_{m}	−0.6192	−0.6192	−0.5710	−0.5363	−0.5363	−0.1869	0.3072*
β ζ_{a}	−0.2243	0.0176	0.0176	0.1415*			
ζ_{m}	−0.4626	−0.4238	−0.1668	0.3300*			
Total energy							
ζ_{a}	−1366.16440						
ζ_{m}	−1363.61822						

Table 3. Comparison of Computed IP by the Koopmans' Theorem of CO-like Electrons in M–CO Cluster with the UPS Data of CO/M Chemisorption System[10—12] (eV)

CO-like	Fe–CO		CO/Fe	Co–CO		CO/Co	Ni–CO		CO/Ni
orbital	ζ_a	ζ_m	Exptl.	ζ_a	ζ_m	Exptl.	ζ_a	ζ_m	Exptl.
4σ	20.48	18.43	17.3	21.99	16.68	16.7	20.75	16.43	16.6
1π	17.08	13.18	13.2	16.46	13.10	13.2	15.52	13.35	13.6
5σ	16.78	14.88	14.4	18.27	12.70	13.8	16.14	12.33	12.3
$\Delta\|4\sigma-1\pi\|$	3.40	5.25	4.1	5.53	3.58	3.5	5.23	3.08	3.0
$\Delta\|5\sigma-1\pi\|$	0.30	1.7	1.2	1.81	0.40	0.6	0.62	1.02	1.3

tendency of CO dissociation. A larger $\Delta|4\sigma-1\pi|$ indicates a larger CO dissociation propensity. The calculations with metallic ζ_m nicely reproduce the experimental trend[13)] that CO dissociatively adsorbed on Fe and associatively adsorbed on Ni, while this is not true for atomic ζ_a. Detailed calculations with metallic ζ_m on CO/Ni and CO/Cu chemisorption systems can be found in Refs. 14 and 15. In Ref. 14, we also discussed the effect of relaxation in light of the more rigorous calculations of Bagus'.[16)]

Shustorovish,[17)] in a paper dedicated to the memory of Muetterties, stated that the modeling is an art that reflects the reality in some surrealistic way, and suggested that the cluster would look like a mermaid, that is part is from molecule and part is from surface. Metallic ζ_m is an example of this "cluster surrealism". Here we give another two examples.

(1) Hermann and Bagus[16)] have carried out the Hartree–Fock calculations for Ni–CO and Ni–N_2, focused on the description of the photoelectron spectra. Significant disagreement with the experimental results led the author to postulate an artificial $3d^94p^1$ configuration for the Ni atom.

(2) Kao and Messmer[18)] has performed the GVB-QCI calculations for Ni–CO (Ni $3d^94s^1$–$3d^{10}$), and compared their results with those of Allison & Goddard's Ni_{14}–CO (Ni $3d^94s^1$) GVB calculation.[19)] Messmer discovered that the failure of Ni_{14}–CO model to describe some of the crucial aspects of the CO/Ni chemisorption is not due to the fact that the cluster size is too small but to the failure to treat the (Ni $3d^94s^1$–$3d^{10}$) energetics properly, and concluded that if electronic correlation effects are properly taken into account, the Ni–CO molecule is an almost *unreasonably* good model for chemisorption!

According to the concept of "metallic atom", the metallic state of Ni is $3d^{9.45}4s^{0.55}$, which is between the $3d^94s^1$–$3d^{10}$ atomic configurations. Thus the electronic correlation of d^9s^1–d^{10} will present a state close to the metallic state of Ni and therefore should be a *reasonably* good model for chemisorption. The energy of 4s orbital in Ni is −7.6 eV, while that of 4p orbital is around −5 eV, comparable to the Fermi level of bulk Ni. Therefore it should be the HF Ni($3d^94p^1$) rather than Ni($3d^94s^1$) which accounts for the chemisorption better.

Choice of Multiplicity. By analogy with the theoretical studies on molecules, people tend to believe that the ground state of a cluster is suitable to model the surface, and the multiplicity of a cluster model is thus that of the ground state cluster. This may be questionable in the cluster-surface analogy. In our opinion, the choice of multiplicity should also be appropriate for bulk metal. For example, the metallic state of Cr is $3d^{5.24}4s^{0.76}$,[20)] which is between the $3d^64s^0$ and $3d^54s^1$ atomic states. $3d^64s^0$ configuration may result in multiplicities of 5, 3, 1; $3d^54s^1$ configuration may result in multiplicities of 7, 5, 3, 1. It is well known that the UHF wavefunctions do not have the full symmetry of the system, and are not the eigenfunctions of an $\hat{S}^2$ operator. The expectation value $\langle\hat{S}^2\rangle$ is larger for a mixture of states of higher spin multiplicity. Thus the UHF wavefunctions of a quintet are mixtures of wavefunctions from quintet and septet rather than a pure quintet; while the UHF wavefunctions of a triplet are mixtures of wavefunctions from triplet, quintet, and septet. This kind of mixture of atomic states is what we expect, for this may mix the atomic states of $3d^64s^0$ and $3d^54s^1$ to give a state close to the metallic state $3d^{5.24}4s^{0.76}$. Therefore a multiplicity of 5 or 3 may be more adequate to the cluster-surface analogy. A multiplicity of 7 is a bias against the mixture of $3d^64s^0$ configuration, while there is no mixture of various spin states in an RHF of singlet. Table 4 illustrates the calculation results with metallic ζ_m for various multiplicities of Cr–CO. Calculation results of multiplicity 5 or 3 do agree better with the experimental results.

According to the metallic configurations from band calculations, the choices of multiplicities in M–CO are listed in parentheses in Table 5. The expectation values of $\langle\hat{S}^2\rangle$ are larger than $S(S+1)$. This is not only due to the mixture of the metal high spin atomic states, but also because of the σ/π

Table 4. Multiplicity Dependency: Comparison between the Calculation Results of Cr–CO Cluster for Various Multiplicities and the Experimental Values[21)]

Multiplicity	1	(3)	(5)	7	Exptl.
CO IP's (eV)					
4σ	18.82	16.80	16.74	17.48	16.6
1π	14.66	12.66	12.60	13.23	
5σ	13.91	11.67	12.03	12.68	12.6
E+1140.0 (au)	−1.0405	−0.9084	−1.2860	−1.2716	
$\langle\hat{S}^2\rangle$	0.00	2.06	6.69	12.06	
$S(S+1)$	0	2	6	12	

Table 5. Choices of the Mulitiplicity

Metal	Metallic configuration[20)]	Atomic configuration	Multiplicity $2S+1$
Cr	$3d^{5.24}4s^{0.76}$	$3d^{6}4s^{0}$–$3d^{5}4s^{1}$	(5), (3), 1—7, 5, 3, 1
Fe	$3d^{7.39}4s^{0.61}$	$3d^{8}4s^{0}$–$3d^{7}4s^{1}$	(3), 1—5, 3, 1
Co	$3d^{8.37}4s^{0.63}$	$3d^{9}4s^{0}$–$3d^{8}4s^{1}$	(2)—4, 2
Ni	$3d^{9.45}4s^{0.55}$	$3d^{10}4s^{0}$–$3d^{9}4s^{1}$	1—(3), 1
Cu	$3d^{10}4s^{1}$	$3d^{10}4s^{1}$	(2)

electron transfers. The 5σ and 2π* orbitals of chemisorbed CO are no longer fully occupied or fully vacant. This is why we choose a multiplicity of 3 in Ni–CO Hartree–Fock calculation. For an MCSCF calculation of Ni–CO, a multiplicity of 1 will result in the mixture between $3d^{10}(^1S)$ and $3d^94s^1(^1D)$, a mechanism not shown in the HF calculation. The idea of mixing the atomic states to approach the corresponding metallic state may provide a simple way to choose the configurations and the configuration coefficients in an MCSCF calculation for the cluster-surface analogy.

With the concept of "metallic atom" in mind, we have carried out a series of calculations [M–CO (M=Cr, Fe, Co, Ni,[14)] Cu[15)]), Ni–L (L=CN, CO, NO),[22)] Pd$_n$–CO (n=1—3)[23)]]. The results turn out to be favorable.

Metallic State Principle. Naturally, bulk metal is produced in a composition process, i.e., starting with a free atom, one obtains the bulk by increasing the size of the cluster. In this synthesis process, it is reasonable to assume that every step in this process is in its ground state, i.e., "ground state atom M···→ground state cluster M$_n$···→bulk M". This is called the "Ground State Principle" in the literature.[24)] In contrast, a bulk metal may be decomposed in the process of "bulk metal···→clusters···→atoms". Suppose that this process is adiabatic, then the electronic properties of bulk metal are retained during this process. In this way, we obtain the so-called metallic clusters and metallic atoms, which differ from bulk metal only in size. Obviously, the metallic clusters are not in their ground states. We call this way to choose the electronic state of M$_n$ cluster the "Metallic State Principle". In the composition process, the separated atomic levels are gradually widened into a band when more atoms are added into the cluster. The band width of M$_n$ gradually approaches to the bulk value with increasing cluster size (Fig. 1). On the other hand, in the adiabatic decomposition process, the band width of an ideal metallic M$_n$ is fixed to be the bulk value. The increase of the number of atoms in the cluster only increases the intensity of the band. Recently, Panas and Siegbahn[25)] have proposed the "Bond-Prepared State Principle". They have had great success in reproducing the chemisorption energy with a cluster of finite size. This is one of the most difficult problems in the cluster-surface analogy. They claimed the Fermi level is of limited importance to the strength of the chemisorption bond, a new picture in cluster modeling of chemisorption. However, we argue that an ideal surface cluster model should guarantee that both M$_n$ cluster approaches to bulk M and M$_n$–L cluster to L/M chemisorption system simultaneously.

Table 6 summarizes the calculation results of Pd$_n$ (n=1—7) clusters (Fig. 2) with $\zeta_{\mathrm{m}}^{\mathrm{ECP}}$.[26)] Because the internal electrons, which are strongly bound to their nuclei, are only slightly perturbed by the presence of the neighboring atoms, they retain much of the character in an isolated atom and are replaced by the Ar core ECP of Wadt and Hay.[27)] The atomic ground state of Pd atom is $^1S(d^{10})$, thus a singlet Pd$_n$ cluster is the most conventional choice.[28,29)] From Table 6, it can be seen that the singlet Pd$_n$ clusters smoothly approach to the bulk with the increasing of the cluster size although the Pd$_7$ cluster is still too small to get converged to the bulk. The electrons in the d orbitals of Pd$_n$ decrease steadily, while those in the sp orbitals increase gradually. The expectation values should be the metallic configuration $4d^{9.63}4s^{0.37}$.[6)] The d levels have been widened into a band. The d-band width of Pd$_7$ is about 4 eV, while the experimental value of bulk Pd is about 5 eV.[7)] The HOMO of Pd$_7$ lies around −8 eV, which should be around −6 eV in the bulk.[7)] As the cluster becomes larger, the energy gap between LUMO and HOMO becomes smaller. This is in accord with the common knowledge that the Fermi level of a conductor can act both as an electron acceptor and an electron donor, and the electron affinity is thus equal to the electron ionization in the bulk. Since there

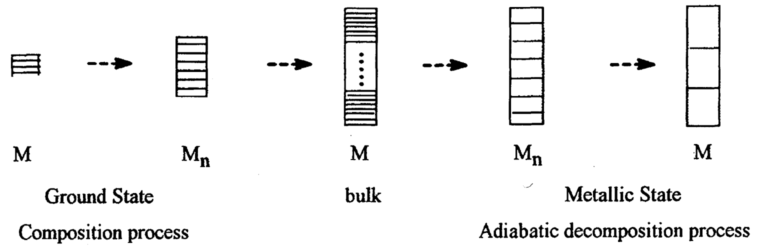

a) b)

Fig. 1. Comparison between the ground state M$_n$ and the metallic state M$_n$. a) In the composition process, the band-width is gradually widened into the bulk value with the increase of the cluster size. b) In the adiabatic decomposition process, the band-width is determined by the character of the bulk. The increase of the cluster size only increases the band density.

Table 6. Calculations for Pd$_n$ Clusters with Metallic ζ_m^{ECP} (au)

Pd$_n$	2S+1=1				2S+1=3			
Clusters	Configurations	d-Band width	HOMO	LUMO	Configurations	d-Band width	HOMO	LUMO
Pd	d^{10}	0.0	−0.3504	0.1953	d^9s^1	0.1174	−0.1935	0.0450
Pd$_2$($D_{\infty h}$)	$d^{9.96}$	0.0719	−0.3185	0.1502	$d^{9.45}s^{0.49}p^{0.06}$	0.2016	−0.1531	−0.0027
Pd$_3$($D_{\infty h}$)	$d^{9.95}$	0.1014	−0.3014	0.1382	$d^{9.62}s^{0.33}p^{0.04}$	0.2181	−0.1790	0.0356
Pd$_3$(D_{3h})	$d^{9.93}$	0.1017	−0.3052	0.1158	$d^{9.60}s^{0.32}p^{0.08}$	0.1587	−0.1625	−0.0289
Pd$_4$(D_{2h})	$d^{9.91}$	0.1141	−0.3016	0.0994	$d^{9.67}s^{0.26}p^{0.08}$	0.2030	−0.1721	−0.0194
Pd$_6$(D_{3h})	$d^{9.90}$	0.1286	−0.2974	0.0841	$d^{9.73}s^{0.19}p^{0.08}$	0.2920	−0.1874	0.0196
Pd$_7$(D_{6h})	$d^{9.88}$	0.1381	−0.2941	0.0743	$d^{9.74}s^{0.17}p^{0.08}$	0.2711	−0.1884	0.0237
Bulk Pd	$d^{9.63}$	0.1837	−0.2205	−0.2205	$d^{9.63}s^{0.37}$	0.1837	−0.2205	−0.2205

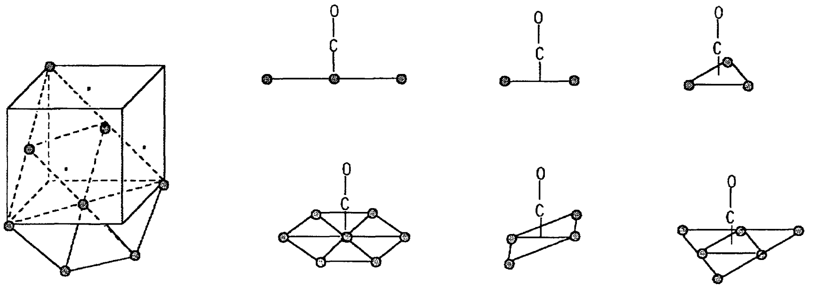

a) b) c) d)

Fig. 2. a) Fcc structure of Pd bulk, the nearest distance between two Pd atoms are 0.275 nm.[5] Cluster models for top-site b), bridge-site c), and hollow-site d) adsorption. (Pd–C 0.193 nm, C–O 0.115 nm[30]).

Table 7. IP's CO-Like Orbitals (eV), C–O Overlap Populations, and Charges on CO in Pd$_n$–CO Experimental IP's of free CO and CO/Pd are also Included.

	4σ	1π	5σ	Δ|4σ−1π|	Δ|4σ−5σ|	Δ|5σ−1π|	C–O	δCO
Free CO	20.48	16.02	13.50	4.46	6.98	2.52	0.502	0.000
2S+1=1								
Top site								
Pd$_3$–CO	20.88	16.43	15.14	4.45	5.74	1.29	0.503	+0.047
Pd$_7$–CO	21.08	16.63	15.44	4.45	5.64	1.19	0.506	+0.063
Bridge site								
Pd$_2$–CO	20.52	16.12	15.46	4.40	5.06	0.67	0.505	+0.021
Pd$_4$–CO	20.69	16.29	15.79	4.40	4.90	0.50	0.507	+0.035
Hollow site								
Pd$_3$–CO	20.48	16.08	15.85	4.40	4.63	0.23	0.507	+0.013
Pd$_6$–CO	20.65	16.24	16.07	4.41	5.58	0.16	0.508	+0.022
2S+1=3								
Top site								
Pd$_3$–CO	17.09	13.33	14.33	3.76	2.76	1.00	0.391	−0.226
Pd$_7$–CO	17.69	14.75	13.49	2.94	4.20	1.26	0.478	−0.119
Bridge site								
Pd$_2$–CO	18.67	14.34	14.82	4.33	3.85	0.48	0.449	−0.215
Pd$_4$–CO	18.89	14.63	14.87	4.26	4.02	0.24	0.463	−0.202
Hollow site								
Pd$_3$–CO	17.97	14.89	14.65	3.08	3.33	0.24	0.424	−0.123
Pd$_6$–CO	18.23	15.16	15.04	3.07	3.19	0.12	0.440	−0.087
Experiment								
Free CO[17]	19.7	16.9	14.0	2.8	5.7	2.9	X	0.0
CO/Pd[30]	17.2	14.2	14.2	3.0	3.0	0.0	$<X$	<0.0

are obvious s occupations in the metallic configuration of bulk Pd, we may choose a multiplicity of 3 for the Pd_n clusters. This means the dissociation limit of Pd_n will be d^9s^1 or $d^9s^1+d^{10}$. The multiplicity of 3 will promote the mixture between d^9s^1 and d^{10}. This may make a small Pd_n cluster more reasonable to simulate the bulk Pd. Table 6 reports the calculation results of Pd_n with the multiplicity of 3. Two important features of data in Table 6 are: That the electronic configurations of triplet Pd_n are closer to that of bulk Pd; and that the d-band widths and the Fermi levels of triplet Pd_n are around 5—6 eV no matter how large the cluster is. The picture of ideal metallic clusters shown in Fig. 1 is roughly reproduced with the triplet Pd_n.

The CO/Pd chemisorption system has been intensively studied both experimentally and theoretically. Our calculation results are summarized in Table 7. As can be seen from Table 7, the qualitative features of the UPS data of CO/Pd(30) are quite well reproduced by the singlet Pd_n–CO clusters. Namely, the $\Delta\,|4\sigma-1\pi|$ remains constant on going from free to adsorbed CO, while $\Delta\,|5\sigma-1\pi|$ decreases considerably. However, the quantitative agreement between theory and experiment is not satisfactory. The computed IP's of singlet Pd_n–CO are all about 2 eV larger than the experimental values. The singlet Pd_n–CO clusters indicate a slightly positively charged CO and a slightly strengthened C–O bond upon CO–Pd_n interaction. This is contrary to the results of work function measurements(31) and IR experiments.(32) The experiments showed a increase of Pd work function upon CO chemisorption, which indicated a negatively charged CO, and a decrease of C–O stretch vibrational frequency, which indicated a weakened C–O bond. An obvious reason which accounts for the failure of the singlet Pd_n–CO is that the Pd_n clusters are too small, so that the computed Fermi levels are too low and the electronic configurations are too close to d^{10}). With the triplet Pd_n–CO clusters, however, all the experimental findings are nicely reproduced.

Concluding Remarks

Our calculation results suggest that a "metallic cluster" may address some of the characteristics in a chemisorption system. However, since we do not perform the ΔSCF calculations, we are not sure whether the better performance of ζ_m is due to error cancellation or the relaxation effect of ζ_m is indeed smaller than that of ζ_a. Clearly, STO-3G is too simple to go into details of a chemisorption system. How to constitute a more reliable metallic basis set of CGTO and how to introduce the concept of "metallic atom" into a post Hartree–Fock calculation are two important tasks for quantitative understanding of chemisorption systems by means of the cluster-surface analogy. Progress has been made on this front.

References

1) E. L. Muetterties and R. M. Wexler, *Surv. Prog. Chem.*, **10**, 61 (1983).

2) S. R. Morrison, "The Chemical Physics of Surface," Plenum, New York (1977), p. 154.

3) N. Wang, X. Xu, and Q. Zhang, *J. Mol. Struct.* (*Theochem.*), **262**, 105 (1992).

4) D. L. Michalopoulos, M. E. Geusic, S. G. Hansen, D. E. Powers, and R. E. Smalley, *J. Chem. Phys.*, **86**, 3914 (1982).

5) A. B. Dai and M. C. Shen, "Periodic Table," Shanghai Science & Technology Press, Shanghai (1981).

6) O. K. Anderson, *Phys. Rev., B*, **B2**, 883 (1970).

7) S. D. Bader, J. M. Blakely, M. B. Brodsky, R. J. Friddle, and R. L. Ponosh, *Surf. Sci.*, **74**, 405 (1978).

8) C. Kittel, "Introduction to Solid State Physics," Wiley, New York (1976), pp. 296—299.

9) W. J. Pietro and W. J. Hehre, *J. Cpmput. Chem.*, **4**, 24 (1983).

10) C. Benndorf, B. Nieber, and B. Kruger, *Surf. Sci.*, **177**, L907 (1986).

11) F. Greuter, D. Heskett, E. W. Plummer, and H. J. Freund, *Phys. Rev., B*, **B27**, 7117 (1983).

12) T. Gustafsson, E. W. Plummer, D. E. Eastman, and J. L. Freedouf, *Solid State Commum.*, **17**, 391 (1975).

13) K. Jagannathan, A. Srinivasan, H. S. Hegde, and C. N. P. Rao, *Surf. Sci.*, **99**, 309 (1980).

14) X. Xu, N. Wang, and Q. Zhang, *Surf. Sci.*, **274**, 378 (1992).

15) X. Xu, N. Wang, and Q. Zhang, *Surf. Sci.*, **274**, 386 (1992).

16) K. Hermann and P. S. Bagus, *Phys. Rev., B*, **B16**, 4195 (1977).

17) E. Shustorovich, in "Quantem Chemistry: The Challenge of Transition Metals and Coordination Chemistry," ed by A. Veillard, Reidel, Dordrecht (1986), p. 461.

18) C. M. Kao and R. P. Messmer, *Phys. Rev., B*, **B31**, 4035 (1985).

19) J. N. Allison and W. A. Goddard, III, *Surf. Sci.*, **115**, 553 (1982).

20) D. H. Xiang, "Solid Catalysis," Chemical Engineering Press, Beijing (1983), p. 122.

21) N. D. Shinn and T. E. Madey, *J. Vac. Sci. Technol., A*, **A4, PtII**, 1351 (1986).

22) X. Xu, N. Wang, and Q. Zhang, *J. Mol. Struct.* (*Theochem.*), **280**, 161 (1993).

23) X. Xu, N. Q. Wang, M. D. Chen, and Q. E. Zhang, *J. Nat. Gas Chem.*, **3**, 231 (1994).

24) I. Panas, P. Siegbahn, and U. Wahlgren, *Theor. Chim. Acta*, **74**, 167 (1988).

25) I. Panas and P. Siegbahn, *J. Chem. Phys.*, **92**, 4625 (1990).

26) ζ_a of Pd atom is from Ref. 9, which is optimized at the d^8s^2 configuration. The Pd_n clusters with ζ_a^{ECP} are strongly bias towards d^8s^2 states, and thus not suitable models to simulate bulk Pd.

27) W. R. Wadt and P. J. Hay, *J. Chem. Phys.*, **82**, 284 (1985).

28) A. Gavezzotti, G. F. Tantardini, and M. Simonetta, *Chem. Phys.*, **105**, 333 (1986).

29) G. Pacchioni and P. S. Bagus, *J. Chem. Phys.*, **93**, 1209 (1990).

30) R. J. Behm, K. Christmann, G. Ertl, and M. A. van Hove, *J. Chem. Phys.*, **73**, 2984 (1980).

31) H. Conrad, G. Ertl, J. Koch, and E. E. Latta, *Surf. Sci.*, **43**, 462 (1974).

32) A. M. Bradshaw and F. M. Hoffmann, *Surf. Sci.*, **72**, 513 (1978).